Displacement of Implant Components from Impressions to Definitive Casts

Sunjai Kim, DDS, PhD[1]/Jack I. Nicholls, PhD[2]/Chong-Hyun Han, DDS, PhD[3]/Keun-Woo Lee, DDS, PhD[4]

Purpose: *Four possible displacements of implant components from a patient model to a definitive cast were assessed to suggest a standard method of comparing the accuracies of implant impression techniques.* ***Materials and Methods:*** *Two techniques for impression making were assessed: a nonsplinted open-tray technique and a light-curing resin splinted open-tray technique. A mandibular model with 5 parallel implants was fabricated. Five definitive casts were fabricated per technique. Using a computerized coordinate measuring machine, 5 part coordinate systems were established, and 7 sets of data were obtained for each sample. From the data, the amount of displacement while connecting components and the linear and angular displacement of components during impression making and cast fabrication were calculated. The Mann-Whitney test was used to determine significant differences between the impression techniques (*$P < .05$*).* ***Results:*** *The average displacements while connecting impression copings and abutment replicas were 31.3 and 30.4 μm, respectively. Less displacement occurred in the nonsplinted group compared to the splinted group during impression making (*$P = .001$*) but greater displacement occurred in that group during definitive cast fabrication (*$P = .015$*).* ***Discussion:*** *In contrast to previous studies, the current study excluded displacement resulting from component connection, because displacement from that source has no relation to impression technique and cannot be controlled.* ***Conclusions:*** *Connecting a component produced as great a displacement as that resulting solely from a impression or cast fabrication. The nonsplinted group was more accurate during impression making but less accurate during cast fabrication.* Int J Oral Maxillofac Implants 2006;21:747–755

Key words: *coordinate measuring machine, displacement, implant, impression*

Recently, nontraditional methods have been introduced to fabricate passive-fitting implant frameworks.[1–3] However, these methods are only useful in refining the fit to the definitive cast. Consequently, the utility of the corrective measures is entirely dependent upon the establishment of an accurate definitive cast. The accuracy of a definitive cast depends on the impression technique, the type of impression material used, and the dimensional accuracy of the material used to fabricate the cast. Numerous studies investigating the accuracy of implant impressions have been published. These studies have described various methods to assess the amount of distortion. Microscopes have been used to compare a reference distance in the patient and in the definitive cast.[4–8] Strain gauges have been used to compare the frequency values produced in a metal framework on the patient and on the definitive cast.[9–13] Photogrammetry, laser videography, and computerized coordinate measuring machines have been used to calculate the Cartesian coordinates and amount of rotational displacement of implant components in the definitive cast.[14–21]

In addition, another consideration affecting the accuracy of the definitive cast is the machining

[1]Assistant Professor, Department of Prosthodontics, Yong-Dong Severance Dental Hospital, College of Dentistry, Yonsei University, Seoul, Korea.
[2]Professor Emeritus, Department of Restorative Dentistry, School of Dentistry, University of Washington, Seattle, Washington.
[3]Professor and Chair, Department of Prosthodontics, Yong-Dong Severance Dental Hospital, College of Dentistry, Yonsei University, Seoul, Korea.
[4]Professor and Chair, Department of Prosthodontics, Dental Hospital, College of Dentistry, Yonsei University, Seoul, Korea.

Correspondence to: Dr Sunjai Kim, Department of Prosthodontics, Yong-Dong Severance Dental Hospital, 146-92 Dogok-dong, Kangnam-gu, Seoul, Korea 135-720. Fax: +082-2-3463-4052. E-mail: sjkimdds@hotmail.com

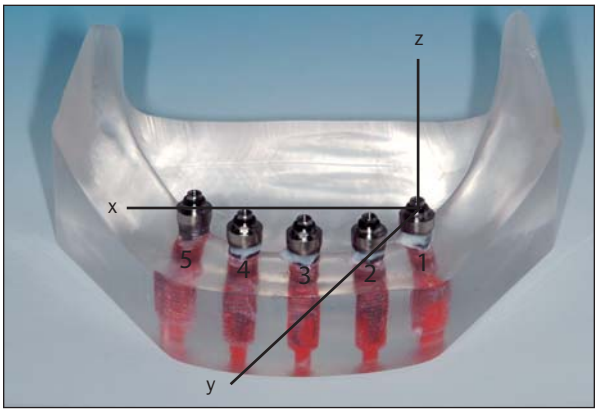

Fig 1 The acrylic resin model. The x, y, and z axes have been superimposed.

tolerances between implant components. Binon reported that machining accuracies were directly related to the location and the magnitude of variation.[22] Ma and associates defined machining tolerance as "the difference in rest positions between the components when these components are held in place by their respective fastening screws."[23] Four kinds of displacement of implant components can be introduced when making a definitive cast. The first is the displacement of each impression coping on the mating surface of each abutment within the range of machining tolerance. The second is the displacement of each impression coping resulting from the impression technique or the material used. The third is the displacement of abutment replicas on the mating surface of each impression coping in the impression tray within the range of machining tolerance. The fourth is the displacement of each abutment replica in the definitive cast because of the dimensional change of the dental stone. Most implant impression studies have compared the difference between the patient and the definitive cast; diverse results have been reported.[5,6,9,10,13] However, to compare the difference between impression techniques, the first and third types of displacement should be excluded, because these displacements did not result from the difference between impression techniques. Moreover, these displacements cannot be controlled. The purpose of the current study was to suggest a standard method for comparing the accuracy of implant impression techniques. For this purpose, 4 areas of possible displacement of implant components were assessed after performing 2 different impression techniques.

MATERIALS AND METHODS

Patient Model Fabrication

An acrylic resin (Lucitone Clear; Dentsply International, York, PA) model of an edentulous mandible was fabricated. Using a dental milling machine (K9; KaVo, Berlin, Germany), 5 parallel holes, 4.25 mm in diameter and 13 mm deep, with centers approximately 8 mm apart, were drilled in the interforaminal area. Five dental implants 4 mm in diameter and 13 mm long (28922; Nobel Biocare, Göteborg, Sweden) were secured in these holes using autopolymerizing acrylic resin (Pattern resin; GC International, Scottsdale, AZ). The screw threads of each 3-mm-collar multiunit abutment (29181; Nobel Biocare) were luted with autopolymerizing resin cement (Panavia 21; Kuraray America, New York, NY) and torqued to 35 Ncm with a manual torque wrench (29165; Nobel Biocare) before cement set. The abutments were numbered 1 through 5, as shown in Fig 1, and the sequence was used throughout the experiment.

Preliminary Cast Fabrication

Five closed-tray impression copings (29090; Nobel Biocare) were hand-screwed to the abutments in the acrylic resin model. An alginate impression (Jeltrate; Dentsply International) of the model was made. After the material had set completely, the impression was removed from the model. Each impression coping was unscrewed, and an abutment replica (RP 29110; Nobel Biocare) was hand-screwed to each impression coping. Each coping/replica assembly was then inserted into the alginate impression to its most stable position. Type III dental stone (Quickstone; Whip Mix, Louisville, KY) was mixed according to the manufacturer's directions and poured into the impression to fabricate the preliminary cast.

Nonsplinted Impression Coping Group

To make a custom tray, 5 open tray impression copings (29089; Nobel Biocare) were hand-tightened to the abutment replicas in the preliminary cast. Two layers of baseplate wax (Truwax; Dentsply Trubyte, York, PA) were placed over the impression copings, and 2 layers of light-curing tray resin (Triad TruTray; Dentsply International) were adapted, trimmed, and light-polymerized on the preliminary cast. A visible light curing unit (Triad 2000; Dentsply International) was used for the polymerization. A window was cut in the tray, exposing the guide pins. The tray was made at least 3 days before final impressions. For the final impression, 5 open-tray impression copings were screwed onto the abutments in the acrylic resin model. Each guide pin was torqued to 10 Ncm with a manual torque wrench (Fig 2).

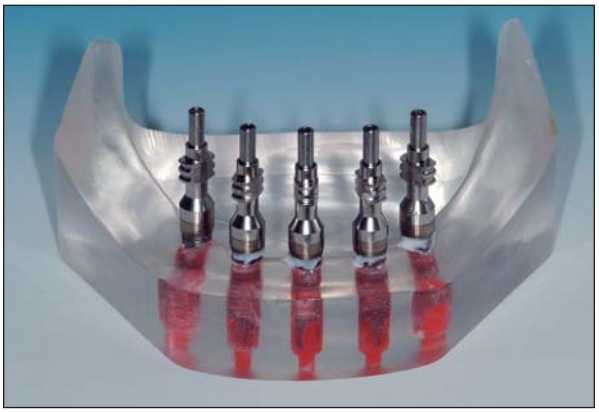

Fig 2 The nonsplinted impression coping group.

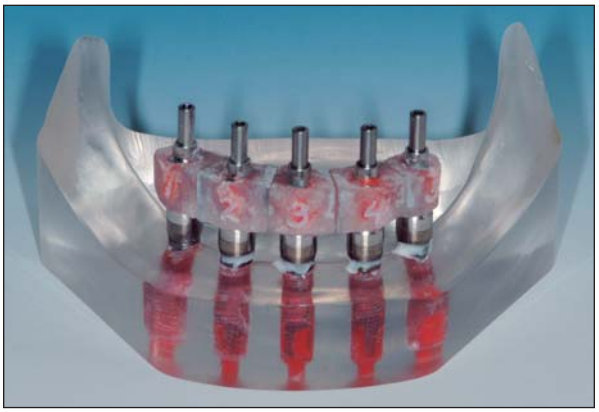

Fig 3 The light-curing resin splinted impression coping group.

Light-Curing Resin Splinted Group

An impression technique introduced by Ivanhoe and associates[24] was slightly modified for this group. A high-viscosity silicone impression material (Express STD Putty; 3M ESPE, St Paul, MN) was used to fabricate a mold to standardize the dimensions of the resin splints. For each resin splint, the mold was placed on the preliminary cast, and 5 open-tray impression copings were hand-tightened onto the abutment replicas in the preliminary cast. A light-curing resin (Triad; Dentsply International, York, PA) was packed around the impression copings and light-polymerized using a light-curing unit (Demetron Optilux 501; Kerr, Romulus, MI). Using the silicone mold, 5 identical resin splints were fabricated. For each resin splint, cuts were made between impression copings using an ultrathin Carborundum disk (Jelenko; Heraeus Kulzer, Hanau, Germany). Each resin splint was segmented into 5 blocks. Each individual resin block was marked to identify its corresponding position. The same method used for the nonsplinted group was used to fabricate a custom tray. For the final impression, the individual resin blocks were secured on the corresponding abutment on the acrylic resin model. A force of 10 Ncm was applied with a manual torque wrench to tighten each guide pin (Fig 3). An adhesive resin (Palavit G LC; Heraeus Kulzer) was applied to wet each cut surface, and a low-viscosity light-curing resin (Palavit G LC K I; Heraeus Kulzer) was used to fill the spaces between the cut surfaces. The buccal and lingual sides of the splinted area were simultaneously exposed to curing lights for 60 seconds. A high-viscosity light-curing resin (Palavit G LC K II; Heraeus Kulzer) was applied and light-polymerized over each splinted area for reinforcement.

Final Impression and Cast Fabrication

Polyether impression material (Impregum Penta; 3M ESPE) was used for final impressions. Polyether adhesive (3M ESPE) was applied to the custom tray 15 minutes before the final impressions were made. Five final impressions were made for each group. One hundred fifty grams of type IV dental stone (FujiRock EP; GC International) was used to fabricate each definitive cast.

Measurements

A computerized coordinate measuring machine (CMM) (Gage 2000; Brown & Sharpe, North Kingston, RI) was used for all the measurements. Each sample underwent 5 measurement phases (Fig 4). All measurements were made by the same operator. The accuracy of the CMM was .005 mm for the x, y, and z axes. Reflex software (Brown & Sharpe) was used for geometric transformation and data processing. The part coordinate system used throughout this study was defined as follows. The centroid of cylinder 1 (the multiunit abutment, impression coping, and abutment replica of implant 1) was designated the origin of the coordinate system. The planar surface of cylinder 1 was regarded as the XY plane. An imaginary line was laid on the ZX plane between the centroid of cylinder 1 and the centroid of cylinder 5. Figure 5 is a schematic drawing of the part coordinate system used. Five different part coordinate systems were established, and 7 sets of data were obtained for each sample. The measuring objects, measuring points, part coordinate systems established, and the meanings of data obtained are described in Tables 1a and 1b.

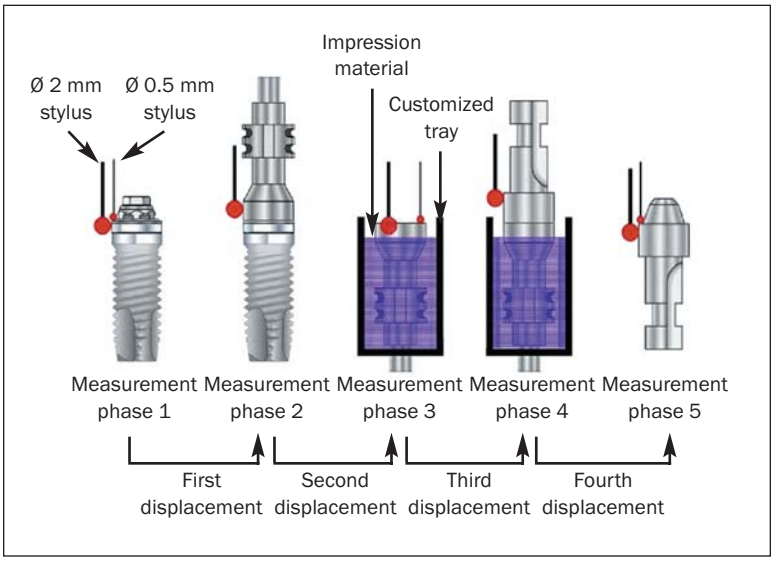

Fig 4 Schematic drawing of the 5 measurement phases.

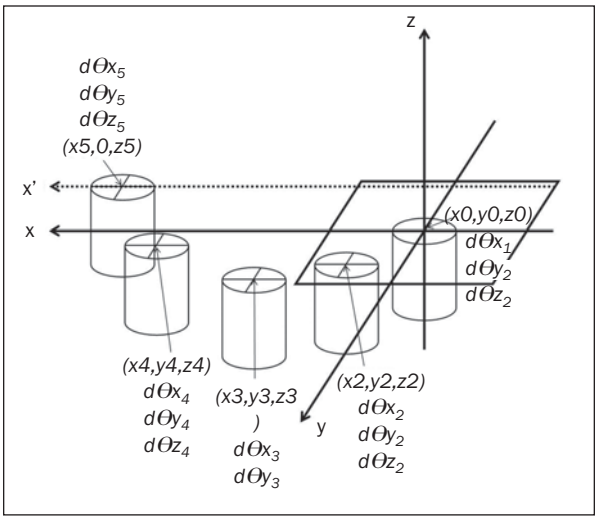

Fig 5 Schematic drawing of the part coordinate system used. X' is an imaginary line which is parallel to the X axis and passes through the centroid of the fifth cylinder.

The entire sequence of measurements is illustrated in Figs 6a through 6g. To facilitate understanding, 3-dimensional conditions have been illustrated 2-dimensionally. The z axis, which is not shown in the figures, was perpendicular to the XY plane. Figure 6a shows the first data set in measurement phase 1. The green circles represent the multiunit abutments in the patient model. By definition, the centroid of multiunit abutment 1 lay on the origin (0, 0, 0), and the centroid of multiunit abutment 5 lay on the ZX plane (x51, 0, z51). The coordinates of the centroids and the angles of tilt of the multiunit abutments were calculated (the first set of data). Figure 6b shows the second data set in measurement phase 2. The blue circles represent the impression copings connected to the multiunit abutment in the patient model. The coordinates of the centroids and the angles of tilt of the impression copings in the first part coordinate system were calculated (the second set of data). As shown in Fig 6b, the coordinates of centroids of impression copings 1 and 5 in the first part coordinate system were (x12, y12, z12) and (x52, y52, z52), respectively. The angles of tilt of the impression copings were equal to the angles of tilt of the multiunit abutments because each impression coping mated with its corresponding abutment. Figure 6c shows the third set of data in measurement phase 2. Using the impression copings, a new part coordinate system (the second) was established. By definition, the centroid of impression coping 1 lay at the origin (0, 0, 0), and the centroid of impression coping 5 lay on the ZX plane (x52*, 0, z52*). Asterisks are used to indicate the same position in different part coordinate systems. The coordinates of other impression copings and the angle of tilt of the impression copings were calculated accordingly (the third set of data). Figure 6d shows the fourth data set in measurement phase 3. The gray circles represent the impression copings in the impression tray. A new part coordinate system (the third) was established in the same manner. The new coordinates of the centroids and the angles of tilt of the impression copings were calculated (the fourth set of data). As before, the centroids of impression copings 1 and 5 were located (0, 0, 0) and (x53, 0, z53), respectively. Figure 6e shows the fifth data set in measurement phase 4. The red circles represent the abutment replicas connected to the impression copings in the impression tray. The coordinates of the centroids and the angles of tilt of the abutment replicas in the impression tray were calculated (the fifth set of data)

Table 1a Five Measurement Phases

Phase	Measuring points*	The part coordinate system established	Obtained data
1	Platform and axial wall of multiunit abutments in the patient model	• The centroid of abutment 1 was established as the origin. • The planar surface of abutment 1 was considered the XY plane. • An imaginary line was laid on the ZX plane between the centroids of abutments 1 and 5.	1. x, y, z coordinates of the centroids and the angles of tilt of the multiunit abutments on the patient model (first set of data)
2	Platform of multiunit abutment and outer axial wall of impression copings in the patient model	• The centroid of impression coping 1 was established as the origin. • The planar surface of abutment 1 was considered the XY plane. • An imaginary line was laid on the ZX plane between the centroids of impression copings 1 and 5.	2. x, y, z coordinates of the centroids and the angles of tilt of the impression copings on the patient model (second set of data) 3. x, y, z coordinates of the centroids and the angles of tilt of the impression copings on the patient model (third set of data)
3	Platforms and inner axial walls of impression copings in the impression tray	• The centroid of impression coping 1 was established as the origin. • The planar surface of impression coping 1 was considered the XY plane. • An imaginary line was laid on the ZX plane between the centroids of impression copings 1 and 5.	4. x, y, z coordinates of the centroids and the angles of tilt of the impression copings in the impression tray (fourth set of data)
4	Platforms of impression copings and axial walls of abutment replicas in the impression tray	• The centroid of abutment replica 1 was established as the origin. • The planar surface of abutment replica 1 was considered the XY plane. • An imaginary line was laid on the ZX plane between the centroids of impression copings 1 and 5.	5. x, y, z coordinates of the centroids and the angles of tilt of the abutment replicas in the impression tray (fifth set of data) 6. x, y, z coordinates of the centroids and the angles of tilt of the abutment replicas in the impression tray (sixth set of data)
5	Platform and axial wall of abutment replicas on the definitive cast	• The centroid of abutment replica 1 was established as the origin. • The planar surface of abutment replica 1 was considered the XY plane. • An imaginary line was laid on the ZX plane between the centroids of abutment replicas 1 and 5.	7. x, y, z coordinates of the centroids and the angles of tilt of the abutment replicas on the definitive cast (seventh set of data)

*Ten points were measured with a 0.5-mm diameter stylus on each planar surface, and 16 points were measured with a 2.0-mm-diameter stylus on each cylinder wall.

Table 1b Comparing the Data Sets to Determine the Amount of Displacement

Difference	Meaning	Mean ± SD
Difference between the first and second sets of data	Displacement of an impression coping on the mating surface of its corresponding abutment	31.3 ± 15.5
Difference between the fourth and fifth sets of data	Displacement of an abutment replica on the mating surface of its corresponding impression coping	30.4 ± 15.6

using the third part coordinate system. The centroids of abutment replicas 1 and 5 were (x14, y14, z14) and (x54, y54, z54), respectively. The angles of tilt of the abutment replicas were equal to the angles of tilt of the impression copings. Figure 6f shows the sixth data set in measurement phase 4. The fourth part coordinate system was established by the abutment replicas in the impression tray according to the definition. The new coordinates of the centroids and the angles of tilt of the abutment replicas were calculated (the sixth set of data). By definition, the centroids of abutment replicas 1 and 5 were (0, 0, 0) and (x54*, 0, z54*), respectively. Figure 6g shows the seventh data set in measurement phase 5. The orange circles represented the abutment replicas in the definitive cast. The fifth part coordinate system was established, and the coordinates of the centroids and

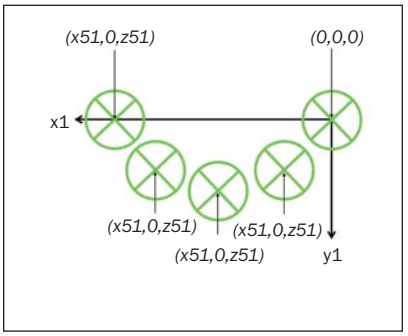

Fig 6a Data set 1.

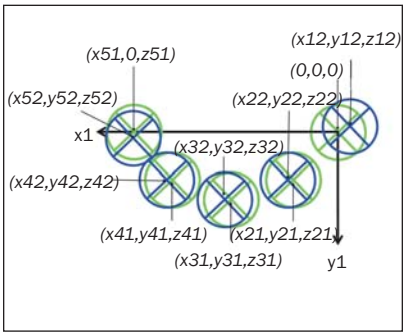

Fig 6b Data set 2.

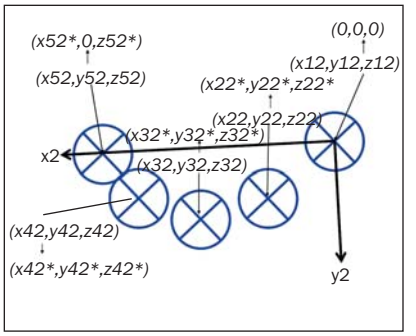

Fig 6c Data set 3.

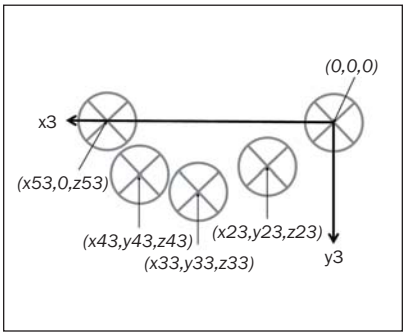

Fig 6d Data set 4.

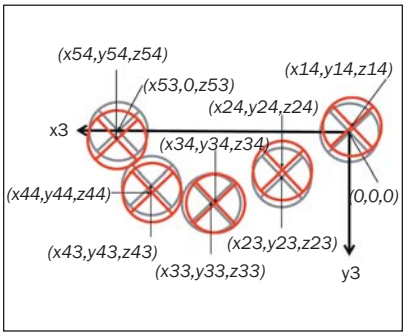

Fig 6e Data set 5.

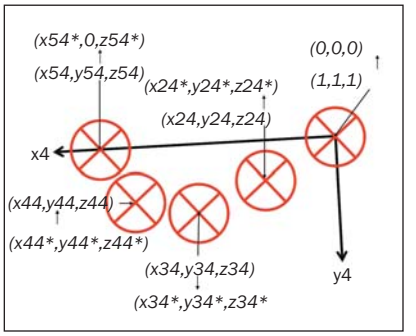

Fig 6f Data set 6.

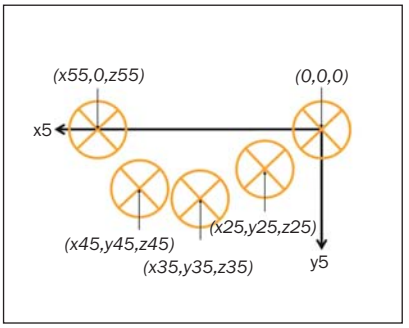

Fig 6g Data set 7.

the angles of tilt of the abutment replicas in the definitive cast were calculated (the seventh set of data). The centroids of abutment replicas 1 and 5 were (0, 0, 0) and (x55, 0, z55), respectively.

Statistical Analysis

The Mann-Whitney test at a confidence level of 95% was used to determine the significance of differences between the 2 groups.

RESULTS

The amount of displacement between an impression coping and the mating surface of its corresponding multiunit abutment was a mean (± SD) of 31.1 (±15.5) μm. This was calculated by comparing the first and second sets of data. The amount of displacement between an abutment replica on the mating surface of its corresponding impression coping was a mean of 30.4 (± 15.6) μm. This was calculated by comparing the fourth and fifth sets of data.

This is the actual amount of distortion resulting from the impression. The displacement of each abutment replica while fabricating a definitive cast was the difference between the coordinates of the centroids and the angles of tilt of the impression copings calculated before (the sixth set of data) and after cast fabrication (the seventh set of data). This is the actual amount of distortion that resulted from the cast fabrication proper. Table2 shows the means, standard deviations, and *P* values for linear and angular distortions for making impressions, fabricating definitive casts, and both impression and cast fabrication procedures. The Δx, Δy, and Δz values are the amounts of displacement of components in the direction of the

Table 2 The Amount of Displacement During Each Procedure

	Linear distortion (μm)				Angular distortion (degree)		
	Mean Δx	Mean Δy	Mean Δz	Mean Δr	ΔΘx	ΔΘy	ΔΘz
Difference between the third and the fourth sets of data (the amount of displacement of each impression coping during impression making)							
Group 1	−3.2 ± 13.9	6.5 ± 21.4	10.3 ± 10.0	23.6 ± 14.2	−0.436 ± 0.071	0.015 ± 0.134	−0.380 ± 0.336
Group 2	−26.0 ± 32.2	0.6 ± 25.2	10.4 ± 9.8	43.7 ± 20.3	−0.404 ± 0.062	−0.015 ± 0.046	−0.272 ± 0.330
P	.01*	.237	.67	.001*	.946	.645	.588
Difference between the sixth and the seventh sets of data (displacement of abutment replica while fabricating the definitive cast)							
Group 1	15.0 ± 9.5	4.0 ± 11.3	−16.8 ± 32.2	36.4 ± 19.2	0.364 ± 0.164	0.085 ± 0.110	0.078 ± 0.216
Group 2	9.5 ± 10.2	1.9 ± 17.6	4.1 ± 8.4	20.7 ± 8.3	0.396 ± 0.075	−0.047 ± 0.036	0.290 ± 0.398
P	.16	.852	.22	.015*	.579	.85	.303
Total amount of displacement from impression and cast fabrication							
Group 1	11.9 ± 16.5	10.5 ± 22.0	−6.5 ± 29.4	36.8 ± 18.5	−0.072 ± 0.141	0.100 ± 0.294	−0.301 ± 0.336
Group 2	−16.5 ± 24.4	2.5 ± 26.2	14.5 ± 12.1	37.6 ± 16.5	−0.008 ± 0.065	−0.062 ± 0.080	0.018 ± 0.293
P	.0007*	.229	.609	.597	.218	.002*	.017*

Group 1 = nonsplinted impression coping group; group 2 = light curing resin splinted impression coping group.
*statistically significant.

axis. Δr was calculated using the equation $\Delta r^2 = \Delta x^2 + \Delta y^2 + \Delta z,^2$ and it represents the 3-dimensional linear displacement of each component. Δθx, Δθy, and Δθz are the amount of the rotation about each X, Y, and Z axis. The amount of displacement while connecting a paired component was as great as the amount of a 3-dimensional linear distortion while making an impression or fabricating a definitive cast. During the impression procedure, the nonsplinted group showed significantly smaller Δr ($P = .001$); however, the light-curing resin splinted group showed significantly smaller Δr ($P = .015$) during the cast fabrication procedure. Considering the total distortion introduced from making an impression to fabricate a definitive cast, there was no significant difference in Δr between the 2 groups ($P = .597$).

DISCUSSION

Various methods have been used to measure the accuracy of implant impression techniques. The unique advantage of a coordinates system is that it is possible to measure the amount of the displacement of a paired component on its mating surface while connecting components. A common part coordinate system in implant accuracy studies is as follows: the centroid of cylinder 1 is designated as the origin, the centroid of cylinder 5 is laid on the X axis, and the centroid of cylinder 3 is laid on the XY plane.[17,19,25,26] Mulcahy and colleagues noted that this part coordinate system could not detect any y-axis or z-axis distortion for cylinder 5 or z-axis distortion for cylinder 3.[27] In the current study, the planar surface of cylinder 1 was designated as the XY plane, and the centroid of cylinder 5 was laid on ZX plane. The main disadvantage of the current part coordinate system is that every coordinate is influenced by the planar surface of cylinder 1. A little angular distortion of cylinder 1 could produce an exaggerated linear and angular distortion of other cylinders. However, the current part coordinate system can detect any distortion except y-axis distortion of cylinder 5. Most importantly, the current part coordinate system corresponds to the "one screw test" which is usually performed to check the fit of a framework in clinical situation.

The amount of the displacement of each impression coping resulting from the impression technique or material used was assessed. For the nonsplinted group, the distortion mainly resulted from the polymerization-related shrinkage of the impression material. In the current study, 5 parallel implants were used, and the nonsplinted group showed smaller Δr compared to the splinted group. However, Phillips and colleagues used a patient model with 5 nonparallel implants and concluded that the amount of the displacement of impression copings between the nonsplinted and the autopolymerized resin splinted groups while making impressions was not statistically different.[19] Feilzer and associates defined the configuration factor or c-factor as the ratio of the bonded to unbonded surface of the restoration[28] and concluded that strong restraint of the bonded walls would cause greater tensile stress in the system.[29] A relatively large c-factor and the restrained resin blocks might cause large tensile strain in the resin splint. It was found that once the guide pins were unscrewed and the impression tray was

removed from the patient model, the strain caused some distortion of the entire resin splint.

The amount of the displacement of each abutment replica while fabricating a definitive cast was assessed. Type IV dental stone has a linear setting expansion of .10% at most.[30] The expansion of dental stone during setting can displace impression coping/abutment replica assemblies. There is very little chance of displacement of the impression coping/abutment replica assemblies because of the setting expansion of dental stone with splinting. The position of each impression coping/abutment replica assembly was maintained only by the impression material in the nonsplinted impression coping group. Even though the polyether impression material is very rigid after setting, the impression coping/abutment replica assemblies can be displaced due to the setting expansion of dental stone.

Considering both the impression and cast fabrication procedure, there was no significant difference in 3-dimensional linear displacement between the 2 impression techniques. The smaller linear displacement of the nonsplinted group during the impression procedure was attenuated by the greater linear displacement in this group during the cast fabrication. However, based on the results of Phillips and colleagues,[19] it can be inferred that splinting may result in less total displacement if the alignment of the implants is not parallel.

Ma and associates[23] reported that the machining tolerances between Brånemark standard abutment components ranged from 22 to 100 μm. Binon reported that the amount of rotational freedom between a Brånemark 3.75-mm-diameter implant and a standard abutment was 6.7 degrees, and the average flat to flat width was 2.707 mm.[22] The amount of gap between the outer axial surface of an external hex and the internal axial surface of an abutment can be calculated by the equation gap = $w \times \cos(30° - \theta)/3.5$ (where w is the flat-to-flat width of external hex and θ is the rotational freedom between components).[31] Based on the equation, the amount of the gap between a Brånemark 3.75-mm-diameter implant and a standard abutment was 82 μm per side. Displacement of a paired component within the range of the gap or the machining tolerance can be introduced during component connection. The present study showed that connecting an impression coping or an abutment replica could introduce more than 30 μm of displacement. This amount is greater than Δr for impressions or cast fabrications in some instances and possibly alters the results of a study designed to investigate the accuracy of different implant impression techniques.

Until now, most of implant accuracy studies compared the definitive cast to the patient model and reported diverse results despite similar experimental designs. These diverse results may have been the result of displacement of a paired component on its mating surface during connecting procedures. In contrast to previous studies, the current study examined solely the amount of displacement of components resulting from the impression technique itself and excluded displacement produced during component connection.

CONCLUSIONS

Within the limitations of this study, it was found that

1. The amount of the displacement of impression copings or abutment replicas that occurred during component connection was as great as the amount of 3-dimensional linear displacement introduced while making impressions or fabricating definitive casts.
2. The nonsplinted group showed smaller 3-dimensional linear distortion than the light-curing resin splinted group during impression-making ($P = .001$).
3. The light-curing resin splinted group showed smaller 3-dimensional linear distortion than the nonsplinted group during the fabrication of definitive casts ($P = .015$).
4. Considering the entire amount of displacement that occurred from impression making to definitive cast fabrication, no significant difference was noted between the impression techniques used ($P = .597$).

ACKNOWLEDGMENTS

The authors thank Nobel Biocare for supplying the implant components for this research. Dr Sunjai Kim specially thanks Dr Jeffrey E. Rubinstein for his support and advice throughout the experiment. This work was supported in part by Yonsei University Research Fund of 2005.

REFERENCES

1. Linehan AD, Windeler AS. Passive fit of implant-retained prosthetic superstructures improved by electric discharge machining. J Prosthodont 1994;3:88–95.
2. Schmitt SM, Chance DA. Fabrication of titanium implant-retained restorations with nontraditional machining techniques. Int J Prosthodont 1995;8:332–336.

3. Eisenmann E, Mokabberi A, Walter MH, Freesmeyer WB. Improving the fit of implant-supported superstructures using the spark erosion technique. Int J Oral Maxillofac Implants 2004;19:810–818.
4. Carr AB. Comparison of impression techniques for a five-implant mandibular model. Int J Oral Maxillofac Implants 1991;6:448–455.
5. Hsu CC, Millstein PL, Stein RS. A comparative analysis of the accuracy of implant transfer techniques. J Prosthet Dent 1993;69:588–593.
6. Herbst D, Nel JC, Driessen CH, Becker PJ. Evaluation of impression accuracy for osseointegrated implant supported superstructures. J Prosthet Dent 2000;83:555–561.
7. Vigolo P, Majzoub Z, Cordioli G. Evaluation of the accuracy of three techniques used for multiple implant abutment impressions. J Prosthet Dent. 2003;89:186–192.
8. Vigolo P, Fonzi F, Majzoub Z, Cordioli G. An evaluation of impression techniques for multiple internal connection implant prostheses. J Prosthet Dent 2004;92:470–476.
9. Assif D, Fenton A, Zarb G, Schmitt A. Comparative accuracy of implant impression procedures. Int J Periodontics Restorative Dent 1992;12:112–121.
10. Inturregui JA, Aquilino SA, Ryther JS, Lund PS. Evaluation of three impression techniques for osseointegrated oral implants. J Prosthet Dent. 1993;69:503–509.
11. Assif D, Marshak B, Schmidt A. Accuracy of implant impression techniques. Int J Oral Maxillofac Implants 1996;11:216–222.
12. Assif D, Nissan J, Varsano I, Singer A. Accuracy of implant impression splinted techniques: Effect of splinting material. Int J Oral Maxillofac Implants 1999;14:885–888.
13. Naconecy MM, Teixeira ER, Shinkai RS, Frasca LC, Cervieri A. Evaluation of the accuracy of 3 transfer techniques for implant-supported prostheses with multiple abutments. Int J Oral Maxillofac Implants 2004;19:192–198.
14. Jemt T. Three-dimensional distortion of gold alloy castings and welded titanium frameworks. Measurements of the precision of fit between completed implant prostheses and the master casts in routine edentulous situations. J Oral Rehabil 1995;22:557–564.
15. Jemt T, Lie A. Accuracy of implant-supported prostheses in the edentulous jaw: Analysis of precision of fit between cast gold-alloy frameworks and master casts by means of a three-dimensional photogrammetric technique. Clin Oral Implants Res 1995;6:172–180.
16. Jemt T. In vivo measurements of precision of fit involving implant-supported prostheses in the edentulous jaw. Int J Oral Maxillofac implants 1996;11:151–158.
17. Jemt T, Rubenstein JE, Carlsson L, Lang BR. Measuring fit at the implant prosthodontic interface. J Prosthet Dent 1996;75:314–325.
18. Riedy SJ, Lang BR, Lang BE. Fit of implant frameworks fabricated by different techniques. J Prosthet Dent 1997;78:596–604.
19. Phillips KM, Nicholls JI, Ma T, Rubinstein J. The accuracy of three implant impression techniques: A three-dimensional analysis. Int J Oral Maxillofac Implants 1994;14:491–495.
20. Lorenzoni M, Pertl C, Penkner K, et al. Comparison of the transfer precision of three different impression materials in combination with transfer caps for the Frialit-2 system. J Oral Rehabil 2000;27:629–638.
21. Akca K, Cehreli MC. Accuracy of 2 impression techniques for ITI implants. Int J Oral Maxillofac Implants 2004;19:517–522.
22. Binon PP. Evaluation of machining accuracy and consistency of selected implants, standard abutments, and laboratory analogs. Int J Prosthodont 1995;8:162–178 [erratum 1995;8:284].
23. Ma T, Nicholls JI, Rubenstein JE. Tolerance measurements of various implant components. Int J Oral Maxillofac Implants 1997;12:371–375.
24. Ivanhoe JR, Adrian ED, Krantz WA. An impression technique for osseointegrated implants. J Prosthet Dent 1991;66:410–411.
25. Tan KB, Rubenstein JE, Nicholls JI, Yuodelis RA. Three-dimensional analysis of the casting accuracy of one-piece, osseointegrated implant-retained prostheses. Int J Prosthodont 1993;6:346–363.
26. Ortorp A, Jemt T, Back T, Jalevik T. Comparisons of precision of fit between cast and CNC-milled titanium implant frameworks for the edentulous mandible. Int J Prosthodont 2003;16:194–200.
27. Mulcahy C, Sherriff M, Walter JD, Fenlon MR. Measurement of misfit at the implant-prosthesis interface: An experimental method using a coordinate measuring machine. Int J Oral Maxillofac Implants 2000;15:111–118.
28. Feilzer AJ, De Gee AJ, Davidson CL. Setting stress in composite resin in relation to configuration of the restoration. J Dent Res 1987;66:1636–1639.
29. Feilzer AJ, De Gee AJ, Davidson CL. Increased wall-to-wall curing contraction in thin bonded resin layers. J Dent Res 1989;68:48–50.
30. Anusavice KJ. Phillips' Science of Dental Materials, ed 11. Philadelphia: Saunders, 2003:338.
31. Kay DA. Trigonometry. New York: John Wiley & Sons, 2001.